



Universiteit  
Leiden  
The Netherlands

## Near-infrared fluorescence imaging with indocyanine green in vascular surgery

Hoven, P. van den

### Citation

Hoven, P. van den. (2022, June 9). *Near-infrared fluorescence imaging with indocyanine green in vascular surgery*. Retrieved from <https://hdl.handle.net/1887/3309684>

Version: Publisher's Version

License: [Licence agreement concerning inclusion of doctoral thesis in the Institutional Repository of the University of Leiden](#)

Downloaded from: <https://hdl.handle.net/1887/3309684>

**Note:** To cite this publication please use the final published version (if applicable).

# Chapter 5

---

## Normalization of time-intensity curves for quantification of foot perfusion using near-infrared fluorescence imaging with indocyanine green

---

P. van den Hoven <sup>1</sup>, F.P. Tange <sup>1</sup>, J.P. van der Valk <sup>1</sup>, N.A. Nerup <sup>2</sup>, H. Putter <sup>1</sup>, C.S.P. Van Rijswijk <sup>1</sup>, J. van Schaik <sup>1</sup>, A. Schepers <sup>1</sup>, A.L. Vahrmeijer <sup>1</sup>, J.E. Hamming <sup>1</sup>, J.R. van der Vorst <sup>1</sup>

1. Leiden University Medical Center, Leiden, The Netherlands
2. Rigshospitalet, Copenhagen, Denmark

*Published in Journal of Endovascular Therapy, March 2022.*

## **Abstract**

### **Introduction**

Near-infrared (NIR) fluorescence imaging using indocyanine green (ICG) is gaining popularity for the quantification of tissue perfusion, including foot perfusion in patients with lower extremity arterial disease (LEAD). However, the absolute fluorescence intensity is influenced by patient – and system related factors limiting reliable and valid quantification. To enhance the quality of quantitative perfusion assessment using ICG NIR fluorescence imaging, normalization of the measured time-intensity curves seems useful.

### **Methods**

In this cohort study, the effect of normalization on two aspects of ICG NIR fluorescence imaging in assessment of foot perfusion was measured: the repeatability and the region selection. Following intravenous administration of ICG, the NIR fluorescence intensity in both feet was recorded for 10 minutes using the Quest Spectrum Platform®. The effect of normalization on repeatability was measured in the non-treated foot in patients undergoing unilateral revascularization pre- and postprocedural (repeatability group). The effect of normalization on region selection was performed in patients without LEAD (region selection group). Absolute and normalized time-intensity curves were compared.

### **Results**

Successful ICG NIR fluorescence imaging was performed in 54 patients (repeatability group, n=38; region selection group, n=16). For the repeatability group, normalization of the time-intensity curves displayed a comparable inflow pattern for repeated measurements. For the region selection group, the maximum fluorescence intensity (Imax) demonstrated significant differences between the three measured regions of the foot ( $p=0.002$ ). Following normalization, the time-intensity curves in both feet were comparable for all three regions.

### **Conclusions**

This study shows the effect of normalization of time-intensity curves on both the repeatability and region selection in ICG NIR fluorescence imaging. The significant difference between absolute parameters in various regions of the foot demonstrates the limitation of absolute intensity in interpreting tissue perfusion. Therefore, normalization and standardization of camera settings are essential steps towards reliable and valid quantification of tissue perfusion using ICG NIR fluorescence imaging.

## Introduction

Near-infrared (NIR) fluorescence imaging has been used as an imaging modality for various indications, including tumor visualization, identification of vital structures and assessment of tissue perfusion (1-4). For the assessment of tissue perfusion, NIR fluorescence imaging has shown potential value in various fields, including vascular -, gastrointestinal - and reconstructive surgery (2, 5, 6). However, there are several factors that influence the stability of the fluorescence intensity which compromise the reliability and validity of the technique, precluding broad application in clinical practice (3, 5). Fluorescence imaging in the NIR light spectrum (700-900nm) has the advantage of high tissue penetration and low autofluorescence, allowing for clear visualization of a fluorophore with an emission peak in the NIR spectrum (7, 8). For the assessment of tissue perfusion, the most utilized fluorophore in NIR fluorescence imaging is indocyanine green (ICG). The feasibility of ICG for assessment of tissue perfusion is explained by the binding to plasma proteins combined with a short half-life due to rapid clearance by the liver (9). Following intravenous administration of ICG, information about tissue perfusion can be obtained using either a qualitative - or quantitative interpretation of the fluorescence intensity. Applications of qualitative interpretation include the assessment of skin viability in reconstructive surgery and the evaluation of bowel perfusion in gastrointestinal surgery (10, 11). However, the qualitative and therefore subjective interpretation of the fluorescence intensity leads to different surgical outcomes and impedes comparison between studies (12). Quantitative assessment of perfusion focuses on describing the fluorescence intensity change over time in a region of interest (ROI), representing the dynamic properties of blood flow (13). Although the benefits of reliable quantitative analysis are evident, several factors influence the stability of the measured fluorescence intensity (3, 8). These factors are either related to the patient or the camera system. Patient related factors include skin type, edema, ICG concentration and the presence of ulcers (14, 15). The change in tissue properties can lead to an alteration in excitation energy and quantum yield, influencing the measured fluorescence intensity (8). Furthermore, the configuration of the camera system affects the measured intensity in several ways, including distance and angle to the target area and optical settings comprising the exposure time and gain (16, 17). This abundance of influencing factors raises questions as to whether analysis of the absolute intensity is appropriate for reliable assessment of tissue perfusion (3, 5). An emerging analyzing method for the assessment of tissue perfusion that adjusts for absolute intensity is normalization (18). Normalization sets the maximum fluorescence intensity at 100% and displays the fluorescence intensity over time as a percentual change. It is hypothesized that this method decreases the influence of beforementioned influencing factors and allows for more reliable and valid quantification. Therefore, the aim of this study was to investigate the influence of normalization on repeatability and region selection of ICG NIR fluorescence imaging for assessment of foot perfusion.

## Methods

This cohort study was approved by the Medical Research and Ethics Committee of the Leiden University Medical Center and registered in the Dutch Trial Register (#NL7531). Patients undergoing unilateral successful revascularization procedures and non-LEAD control patients were included. Patients were included in a single academic hospital in the Netherlands from December 2018 until April 2021. Patients were excluded based on contra-indications to ICG: allergy or hypersensitivity to ICG or (sodium) iodide; hyperthyroidism, autonomous thyroid adenoma, pregnancy, kidney failure (eGFR <45) or severe liver failure. Informed consent was obtained from all individual participants included in the study.

### ICG NIR fluorescence imaging

ICG NIR fluorescence imaging measurements were performed using the Quest Spectrum Platform<sup>®</sup> (Quest Medical Imaging, Middenmeer, The Netherlands). This system consists of a LED laser combined with a camera measuring light in the visible and NIR light spectrum (700-900nm). All patients underwent ankle-brachial index (ABI) - and toe pressure (TP) measurements prior to the ICG NIR fluorescence imaging measurement. Upon ICG (VERDYE 25 mg, Diagnostic Green GmbH, Aschheim-Dornach, Germany) administration, the camera registered the NIR fluorescence intensity change over time in both feet for 10 minutes. All measurements were performed with the patient in a supine position in a darkened room. The camera was placed at approximately 50cm of the foot, perpendicular to the dorsum of the foot. All videos were recorded using an exposure time of 145 milliseconds and a gain of 22 decibel.

### Repeatability group

The effect of normalization on repeatability was measured in the non-treated foot of patients undergoing unilateral revascularization. It was hypothesized that the time-intensity curves in the non-treated contralateral foot remained unchanged. A subset of this group was described in an earlier study in which only normalized data was used (19). ICG NIR fluorescence imaging was performed before – and after the procedure (<3 days) and patients were administered an intravenous bolus injection of 0.1 mg/kg ICG. Three ROIs were analyzed: 1. The dorsum of the foot, 2. The forefoot and 3. The hallux.

### Region selection group

The effect of normalization on region selection was measured in non-LEAD control patients, since this group is most likely to display a homogenous perfusion pattern in various regions of the foot. This group consisted of patients undergoing liver metastasectomy who were administered ICG intravenously 1 day before surgery. In this

group, a bolus injection of 10mg ICG was administered intravenously as part of the non-investigational treatment protocol. Three regions were selected based on differences in camera distance and angle of the surface area to the camera. These regions included: 1. The hallux, 2. The first ray of the foot and 3. The lateral foot.

### **Data analysis**

The Quest Research Framework® (Quest Medical Imaging, Middenmeer, the Netherlands) software was used for the quantification of the measured NIR fluorescence intensity. Following manual selection of an ROI, the software creates a curve of the fluorescence intensity change over time. The measured fluorescence intensity is displayed as arbitrary units (a.u.). When normalization is applied, the software sets the maximum fluorescence intensity in the selected ROI at 100% and displays the fluorescence intensity over time as a percentual change of this maximum fluorescence. The absolute time-intensity curves and normalized time-intensity curves with the extracted parameters are displayed in Supplementary Figure 1 and Supplementary Table 1. After normalization, absolute parameters including ingress and ingress rate are depleted. The normalized slope for the ingress and egress are defined as percentage per second. A tracker was used to ensure the ROI was synchronized with foot movement and baseline subtraction was applied. Starting time of the time-intensity curves was defined as an increase of 1 arbitrary unit for the absolute time-intensity curves and 1% for the normalized time-intensity curves. Statistical analyses were performed using IBM SPSS Statistics 25 (IBM Corp. Released 2017. IBM SPSS Statistics for Windows, Version 25.0. Armonk, NY, USA: IBM Corp.). Parameters in the repeatability group were compared with the Wilcoxon rank sign test for paired analyses. Results for the region selection group were compared using the Kruskal-Wallis test.

### **Results**

ICG NIR fluorescence imaging was successfully performed in 54 patients. The patient characteristics for both the repeatability group and region selection group are displayed in Table 1. In the repeatability group, consisting of 38 patients, the mean age was 70.9 years with a standard deviation (SD) of 7.0. The mean ABI in this group was 0.89 (SD 0.30). with a mean TP of 76 mmHg (SD 30). The 16 patients (32 limbs) in the region selection group displayed a mean age of 66.6 years (SD 12.3) with a mean ABI of 1.11 (SD 0.10) and a mean TP of 106 mmHg (SD 22).

Table 1. Patient characteristics.

|                          | Repeatability group (n=38) | Region selection group (n=16) |
|--------------------------|----------------------------|-------------------------------|
| Age in years (SD)        | 70.9 (7.0)                 | 66.6 (12.3)                   |
| Female, n(%)             | 17 (44.7)                  | 3 (18.8)                      |
| Diabetes, n(%)           | 12 (31.6)                  | 3 (18.8)                      |
| Hypertension, n(%)       | 29 (76.3)                  | 7 (43.8)                      |
| Active smoking, n(%)     | 8 (21.1)                   | 1 (6.3)                       |
| History of smoking, n(%) | 35 (92.1)                  | 10 (62.5)                     |
| Mean baseline ABI (SD)   | 0.89 (0.30)                | 1.11 (0.10)                   |
| Mean baseline TP (SD)    | 76 (30)                    | 106 (22)                      |

Abbreviations: SD, standard deviation; TP, toe pressure; ABI, ankle-brachial index.

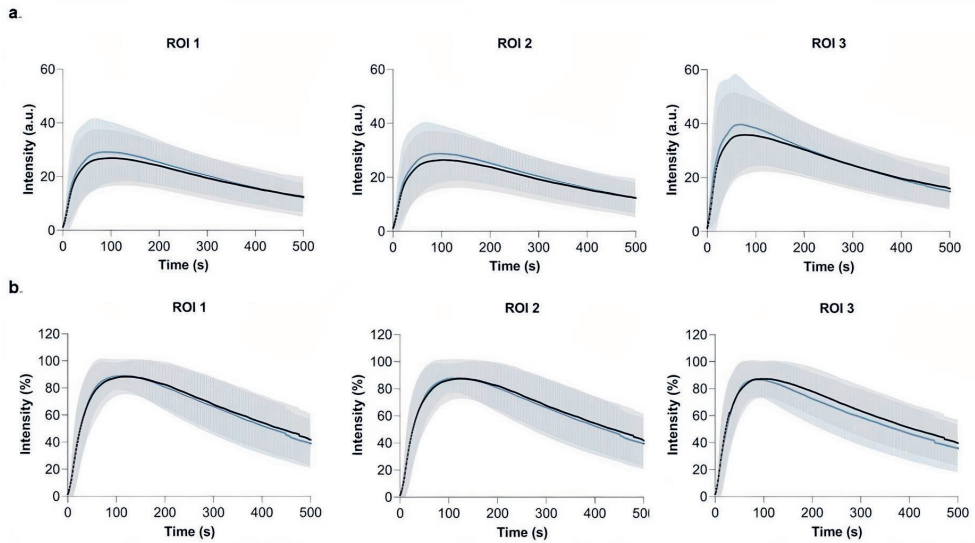
### Repeatability group

For the repeatability group, no significant differences were found for the ABI and TP pre- and post-procedural (ABI: 0.89 vs. 0.86,  $p=0.806$ ; TP: 76 vs. 72,  $p=0.466$ ). The results on repeated measurements for both the absolute and normalized time-intensity curves in the repeatability group are displayed in Figure 1. For the absolute time-intensity curves, an increase in maximum fluorescence intensity ( $I_{max}$ ) is seen for all three ROIs for the repeated measurements. Furthermore, the absolute time-intensity curves in ROI 3 display a wider distribution compared to the other ROIs. After normalization, the time-intensity curves display a similar distribution amongst all three ROIs. Furthermore, the inflow pattern is comparable for repeated measurements. The results on quantification of the time-intensity curves for the repeatability group are depicted in Table 2. Except for the area under the curve (AUC) ingress in ROI 3, no statistical differences were found for all measured parameters in all ROIs. Although not significant, absolute parameters including the  $I_{max}$ , ingress rate and slope were higher for the repeated measurement. For the ingress rate in ROI 1 and 2, the repeated measurement displayed a fifty percent increase (ROI1: 0.4 vs 0.6,  $p=0.587$ , ROI 2: 0.4 vs. 0.6,  $p=0.404$ ). After normalization, the slope in all ROIs were comparable (ROI 1: 3.4 vs. 3.5,  $p=0.983$ , ROI 2: 3.4 vs. 3.4,  $p=0.936$ , ROI 3: 0.8 vs 1.0,  $p=0.502$ ).

### Region selection group

The absolute and normalized time-intensity curves for the region selection group are visualized in Figure 2. Results for the right- and left foot are displayed separately. For the absolute time-intensity curves, there is a clear discrepancy for the measured maximum fluorescence intensity between the three ROIs. The lowest maximum intensity is seen in ROI 3, i.e. the lateral foot, which is visualized in Figure 3. Furthermore, there is a wide distribution amongst all three measured ROIs. After normalization, the patterns observed in both the right and left foot are comparable for all three ROIs. The extracted parameters for the region selection group are displayed in Table 3. For the fixed

parameters, no significant differences were found for all three ROIs in both feet. For the absolute parameters, a statistical significance was seen for the  $I_{max}$ , ingress rate and slope ingress in the right as well as the left foot (right:  $p=0.002, 0.015, 0.005$ ; left:  $p=0.006, 0.011, 0.037$ , respectively). After normalization, a significant difference was seen for the slope egress in both feet (right:  $p<0.001$ , left:  $p<0.001$ ). The normalized ingress slope was comparable for all ROIs (right:  $p=0.408$ , left  $p=0.921$ ).



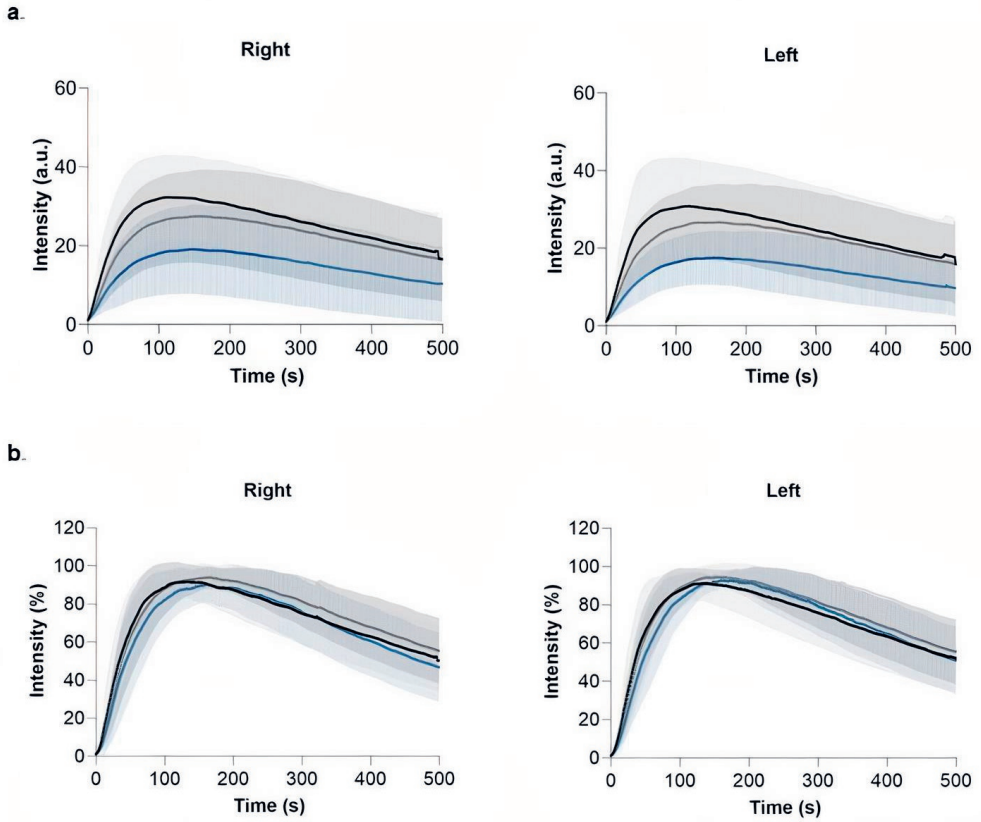
**Figure 1.** Repeatability group - absolute (a) and normalized (b) time-intensity curves for the three ROIs of the foot pre- (black line) and post-revascularization (blue line). Results are displayed as mean (bold line) with one standard deviation distribution.



Table 2. Repeatability group – ICG NIR fluorescence imaging outcome.

|  | Mean ± SD    | Mean ± SD    |       |              |              |             |             |             |           |           |           |           |           |
|--|--------------|--------------|-------|--------------|--------------|-------------|-------------|-------------|-----------|-----------|-----------|-----------|-----------|
| <b>ABI</b>                             | 0.89 ± 0.30  | 0.86 ± 0.33  | 0.806 |              |              |             |             |             |           |           |           |           |           |
| <b>TP</b>                              | 76 ± 30      | 72 ± 27      | 0.466 |              |              |             |             |             |           |           |           |           |           |
|  |              |              |       | <b>ROI1</b>  |              | <b>ROI2</b> |             | <b>ROI3</b> |           |           |           |           |           |
|  |              |              |       | Pre          | Post         | Pre         | Post        | Pre         | Post      | Pre       | Post      | Pre       | Post      |
|  |              |              |       | Mean ± SD    | Mean ± SD    | Mean ± SD   | Mean ± SD   | Mean ± SD   | Mean ± SD | Mean ± SD | Mean ± SD | Mean ± SD | Mean ± SD |
| <b>ICG NIR fluorescence parameters</b> |              |              |       |              |              |             |             |             |           |           |           |           |           |
| <b>Tmax</b>                            | 111.8 ± 68.1 | 102.8 ± 61.3 | 0.346 | 115.1 ± 67.8 | 103.8 ± 60.9 | 0.218       | 90.1 ± 58.1 | 75.0 ± 48.4 | 0.177     |           |           |           |           |
| <b>AUC10</b>                           | 47.6 ± 2.3   | 47.4 ± 1.9   | 0.733 | 47.5 ± 2.8   | 47.3 ± 2.0   | 0.538       | 47.6 ± 2.7  | 47.7 ± 4.6  | 0.922     |           |           |           |           |
| <b>AUC ingress</b>                     | 71.6 ± 4.9   | 70.6 ± 5.6   | 0.538 | 70.9 ± 5.5   | 69.5 ± 5.8   | 0.438       | 70.0 ± 5.6  | 66.5 ± 7.9  | 0.028     |           |           |           |           |
| <b>AUC egress 60</b>                   | 95.2 ± 4.5   | 94.8 ± 4.1   | 0.879 | 95.0 ± 4.9   | 94.8 ± 4.8   | 0.567       | 93.5 ± 5.8  | 91.8 ± 7.8  | 0.331     |           |           |           |           |
| <b>AUC egress 120</b>                  | 90.2 ± 6.8   | 89.5 ± 6.6   | 0.617 | 89.7 ± 7.5   | 89.3 ± 6.9   | 0.500       | 87.8 ± 8.5  | 85.4 ± 10.2 | 0.242     |           |           |           |           |
| <b>AUC egress 180</b>                  | 84.9 ± 8.4   | 83.9 ± 8.3   | 0.645 | 84.3 ± 9.0   | 83.5 ± 8.5   | 0.521       | 82.4 ± 9.9  | 79.8 ± 11.5 | 0.172     |           |           |           |           |
| <b>AUC egress 240</b>                  | 79.5 ± 9.4   | 78.5 ± 9.5   | 0.626 | 79.2 ± 10.0  | 78.4 ± 9.7   | 0.572       | 77.6 ± 10.6 | 74.4 ± 12.2 | 0.177     |           |           |           |           |
| <b>AUC egress 300</b>                  | 74.6 ± 10.2  | 69.9 ± 12.8  | 0.623 | 73.9 ± 10.7  | 73.2 ± 10.5  | 0.578       | 72.6 ± 10.9 | 69.9 ± 12.8 | 0.172     |           |           |           |           |
| <b>Imax</b>                            | 30.0 ± 10.8  | 32.9 ± 13.5  | 0.286 | 29.7 ± 10.8  | 32.9 ± 12.6  | 0.204       | 41.2 ± 16.7 | 47.1 ± 22.2 | 0.187     |           |           |           |           |
| <b>Ingress rate</b>                    | 0.4 ± 0.5    | 0.6 ± 0.8    | 0.587 | 0.4 ± 0.5    | 0.6 ± 0.7    | 0.404       | 0.8 ± 0.9   | 1.2 ± 1.6   | 0.150     |           |           |           |           |
| <b>Absolute slope ingress</b>          | 1.1 ± 0.9    | 1.4 ± 1.5    | 0.528 | 1.1 ± 0.8    | 1.4 ± 1.4    | 0.293       | 1.9 ± 1.8   | 2.7 ± 3.0   | 0.158     |           |           |           |           |
| <b>Absolute slope egress</b>           | 0.3 ± 0.1    | 0.3 ± 0.2    | 0.833 | 0.2 ± 0.1    | 0.3 ± 0.1    | 0.350       | 0.3 ± 0.2   | 0.5 ± 0.5   | 0.133     |           |           |           |           |
| <b>Normalized slope ingress</b>        | 3.4 ± 2.0    | 3.5 ± 2.4    | 0.983 | 3.4 ± 2.0    | 3.4 ± 2.3    | 0.936       | 4.1 ± 2.4   | 4.5 ± 2.9   | 0.656     |           |           |           |           |
| <b>Normalized slope egress</b>         | 0.8 ± 0.4    | 0.8 ± 0.5    | 0.547 | 0.8 ± 0.4    | 0.7 ± 0.3    | 0.313       | 0.8 ± 0.4   | 1.0 ± 0.7   | 0.502     |           |           |           |           |

Abbreviations: SD, standard deviation; TP, toe pressure; ABI, ankle brachial index; AUC, area under the curve.



**Figure 2.** Region selection group - absolute (a) and normalized (b) time-intensity curves for the right and left foot displaying the hallux region (black line), first ray region (grey line) and lateral foot region (blue line). Results are displayed as mean (bold line) with one standard deviation distribution.

Table 3. Region selection group - ICG NIR fluorescence imaging outcome.

| <i>ICG NIR fluorescence parameters</i> | Right foot                |                           |                           | Left foot                 |                           |                           | <b>P</b> |
|--|---------------------------|---------------------------|---------------------------|---------------------------|---------------------------|---------------------------|----------|
|  | <b>ROI 1</b>              | <b>ROI 2</b>              | <b>ROI 3</b>              | <b>ROI 1</b>              | <b>ROI 2</b>              | <b>ROI 3</b>              |          |
| <b>Tmax</b>                            | Mean ± SD<br>157.7 ± 69.4 | Mean ± SD<br>161.7 ± 69.8 | Mean ± SD<br>126.2 ± 64.6 | Mean ± SD<br>157.5 ± 74.9 | Mean ± SD<br>153.5 ± 72.6 | Mean ± SD<br>124.3 ± 73.5 | 0.341    |
| <b>AUC10</b>                           | 50.0 ± 5.0                | 48.7 ± 4.7                | 49.8 ± 5.2                | 48.9 ± 6.3                | 49.3 ± 6.0                | 50.9 ± 6.4                | 0.547    |
| <b>AUC ingress</b>                     | 72.5 ± 5.3                | 68.7 ± 4.7                | 69.8 ± 5.7                | 72.2 ± 4.0                | 67.8 ± 5.0                | 69.5 ± 4.2                | 0.039    |
| <b>AUC egress 60</b>                   | 96.9 ± 2.0                | 95.8 ± 1.9                | 96.2 ± 2.7                | 97.1 ± 1.9                | 95.0 ± 4.1                | 96.0 ± 2.8                | 0.140    |
| <b>AUC egress 120</b>                  | 93.3 ± 3.1                | 91.9 ± 3.2                | 91.8 ± 4.7                | 93.6 ± 2.5                | 90.7 ± 4.9                | 91.8 ± 4.8                | 0.287    |
| <b>AUC egress 180</b>                  | 89.1 ± 4.5                | 87.1 ± 4.6                | 87.4 ± 6.1                | 89.4 ± 3.5                | 85.6 ± 5.5                | 87.5 ± 6.2                | 0.169    |
| <b>AUC egress 240</b>                  | 84.9 ± 5.6                | 81.6 ± 5.0                | 83.0 ± 7.1                | 85.1 ± 4.4                | 79.9 ± 5.8                | 83.3 ± 7.1                | 0.061    |
| <b>AUC egress 300</b>                  | 80.3 ± 6.0                | 76.9 ± 5.7                | 78.2 ± 7.6                | 80.3 ± 5.0                | 74.7 ± 6.3                | 78.5 ± 7.4                | 0.065    |
| <b>Imax</b>                            | 28.4 ± 18.8               | 18.9 ± 7.8                | 33.7 ± 14.3               | 29.3 ± 12.8               | 21.1 ± 12.1               | 35.2 ± 11.8               | 0.006    |
| <b>Ingress rate</b>                    | 0.2 ± 0.1                 | 0.1 ± 0.1                 | 0.4 ± 0.4                 | 0.2 ± 0.1                 | 0.2 ± 0.1                 | 0.4 ± 0.3                 | 0.011    |
| <b>Absolute slope ingress</b>          | 0.7 ± 0.4                 | 0.4 ± 0.2                 | 1.0 ± 0.7                 | 0.7 ± 0.4                 | 0.6 ± 0.4                 | 1.0 ± 0.7                 | 0.037    |
| <b>Absolute slope egress</b>           | 0.2 ± 0.1                 | 0.2 ± 0.1                 | 0.2 ± 0.1                 | 0.2 ± 0.1                 | 0.2 ± 0.1                 | 0.2 ± 0.1                 | 0.104    |
| <b>Normalized slope ingress</b>        | 2.4 ± 0.8                 | 2.2 ± 0.6                 | 2.8 ± 1.3                 | 2.4 ± 0.8                 | 2.7 ± 1.5                 | 2.9 ± 1.9                 | 0.921    |
| <b>Normalized slope egress</b>         | 0.7 ± 0.3                 | 1.2 ± 0.5                 | 0.6 ± 0.2                 | 0.6 ± 0.3                 | 1.2 ± 0.5                 | 0.6 ± 0.2                 | <0.001   |

Abbreviations: SD, standard deviation; AUC, area under the curve.

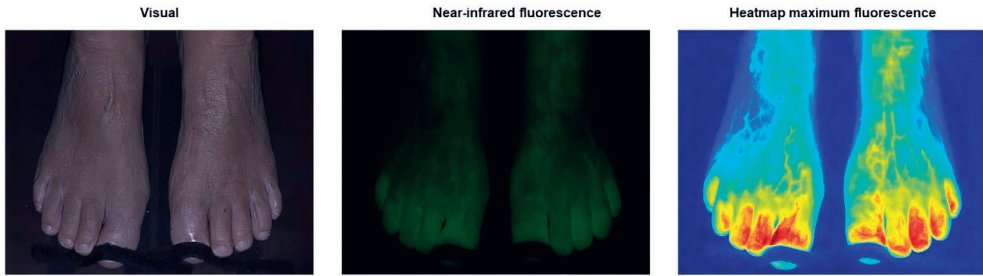


**Figure 3.** Output of the Quest Research Framework® showing the visual light (left), near-infrared fluorescence (middle) and heatmap of the maximum fluorescence intensity (right) of a 70-year old female control patient. The heatmap illustrates the diminished observed maximum fluorescence intensity found on the lateral side of the foot.

## Discussion

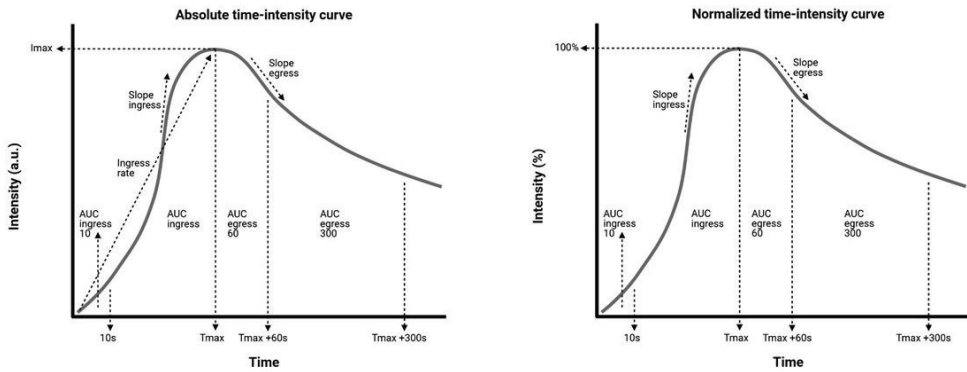
This study demonstrates the effect of normalization of time-intensity curves on both the repeatability and region selection in the quantification of tissue perfusion using ICG NIR fluorescence imaging. Concerning repeatability, time-intensity curves display a more similar pattern following normalization. Although not significant, absolute parameters including ingress rate and slope varied between measurements and displayed a wider distribution. These findings suggest that absolute parameters are less reliable and more susceptible to fluctuations on repeated measurements. The repeatability of ICG NIR fluorescence imaging for assessment of tissue perfusion in patients with LEAD was described in one earlier study (20). This study found time-intensity curves to be repeatable and focused on time- as well as absolute parameters. However, repeated measurements were performed in the same setting by the same investigator, thus reducing the impact of influencing factors of measurement setup on the NIR signal. Regarding the region selection, absolute inflow parameters in the present study were all significantly different between various areas of the foot. After normalization, the slope ingress was comparable. For the interpretation of tissue perfusion with ICG NIR fluorescence imaging, these are important findings, since absolute parameters can thus lead to an incorrect interpretation of actual tissue perfusion. In the search for reliable quantification of tissue perfusion with ICG NIR fluorescence imaging, an abundance of parameters have been studied in various target tissues (13). For the quantification of skin perfusion in patients with LEAD for example, time-related and normalized parameters appear to be superior to measurements of maximum intensity (21, 22). In reconstructive surgery, a commonly performed analyzing method for tissue quantification is the use of relative parameters (6). However, this method does not take into account the camera angle and distance, leading to a misperception of actual

perfusion. In gastro-intestinal surgery, the effect of normalization on quantification of bowel perfusion was measured in several studies (3, 18, 23). In a series of studies by Nerup et al. on gastrointestinal perfusion in porcine models, the normalized slope ingress was significantly correlated with regional blood flow and local lactate levels (18, 23). Although reliable quantification of tissue perfusion seems to tend towards the use of normalized parameters, several items have to be discussed. First of all, normalization of the time-intensity curves leads to alteration of data, which precludes the use of absolute parameters that can be useful in the prediction of tissue necrosis (24). Furthermore, normalization can be unreliable when the measured fluorescence intensity levels are below a certain threshold. Magnification of the signal can then lead to high fluctuations in the percentual change, which is the presumable cause of the significant increase in normalized egress slope in the region selection group in this study. In addressing the effect of normalization on region selection, the cohort in this study consisted of patients without known LEAD who were administered ICG as part of the treatment protocol for liver metastasectomy. By selecting this group of patients, this study avoided the exposure of healthy volunteers to ICG. However, due to comorbidities, there might have been changes in regional circulation of the foot that could have influenced the measured fluorescence intensity. Therefore, future studies on ICG NIR fluorescence imaging for foot perfusion assessment should ideally be performed in a control group that has a significantly lower risk of possible unknown underlying LEAD. Concerning the repeatability group, this study is limited by the small sample size. Besides, measurements were performed on different days post-procedural, which might have led to inter-patient variability. Furthermore, changes in hemodynamic status, including blood pressure and pulse could have influenced the measured fluorescence intensity (25). Despite these limitations, the present study describes a new perspective on assessment of tissue perfusion in the foot using ICG NIR fluorescence imaging. Improving reliability and validity of ICG NIR fluorescence imaging in quantification of tissue perfusion using normalization can promote comparability between studies. To compare standardized quantification methods between studies, it is also of paramount importance to report on the used camera system and - settings, including exposure time and gain. Addressing these aspects in future studies on perfusion assessment using ICG NIR fluorescence imaging is an essential step towards reliable quantification. Whether this quantification will lead to a better understanding of actual in- and outflow of foot perfusion has yet to be determined. However, reliable quantification will be a crucial factor in the value of future studies on perfusion assessment with ICG NIR fluorescence imaging. Therefore, normalization should be a standard procedure in the analysis of the measured fluorescence intensity in these studies. The valid and reliable assessment of tissue perfusion using ICG NIR fluorescence imaging could then potentially aid in the prediction of clinical outcome following revascularization or in assessing the probability of wound healing.

## Conclusion

This study shows the effect of normalization of time-intensity curves on both the repeatability and region selection for the quantification of foot perfusion using ICG NIR fluorescence imaging. The significant difference between absolute parameters in various regions of the foot demonstrates the limitation of absolute intensity in interpreting tissue perfusion. Therefore, normalization and standardization of camera settings are essential steps towards reliable and valid quantification of tissue perfusion using ICG NIR fluorescence imaging.

# Appendices



**Supplementary Figure 1.** Absolute (left) and normalized (right) time-intensity curves with extracted parameters.

**Supplementary Table 1.** ICG NIR fluorescence imaging parameters.

| Fixed parameters   | Absolute parameters    | Normalized parameters |
|--------------------|------------------------|-----------------------|
| Tmax (s)           | Imax (a.u.)            | Slope ingress (%/s)   |
| AUC10 (%)          | Ingress rate (a.u./s)  | Slope egress (%/s)    |
| AUC ingress (%)    | Slope ingress (a.u./s) |                       |
| AUC egress 60 (%)  | Slope egress (a.u./s)  |                       |
| AUC egress 120 (%) |                        |                       |
| AUC egress 180 (%) |                        |                       |
| AUC egress 240 (%) |                        |                       |
| AUC egress 300 (%) |                        |                       |

Abbreviations: s, seconds; AUC, area under the curve; a.u., arbitrary unit(s).

## Reference list

1. de Valk KS, Handgraaf HJ, Deken MM, Sibinga Mulder BG, Valentijn AR, Terwisscha van Scheltinga AG, et al. A zwitterionic near-infrared fluorophore for real-time ureter identification during laparoscopic abdominopelvic surgery. *Nat Commun.* 2019;10(1):3118.
2. van den Hoven P, Ooms S, van Manen L, van der Bogt KEA, van Schaik J, Hamming JF, et al. A systematic review of the use of near-infrared fluorescence imaging in patients with peripheral artery disease. *J Vasc Surg.* 2019;70(1):286-97 e1.
3. Lutken CD, Achiam MP, Svendsen MB, Boni L, Nerup N. Optimizing quantitative fluorescence angiography for visceral perfusion assessment. *Surg Endosc.* 2020;34(12):5223-33.
4. Schaafsma BE, Mieog JS, Hutteman M, van der Vorst JR, Kuppen PJ, Lowik CW, et al. The clinical use of indocyanine green as a near-infrared fluorescent contrast agent for image-guided oncologic surgery. *J Surg Oncol.* 2011;104(3):323-32.
5. Slooter MD, Mansvelders MSE, Bloemen PR, Gisbertz SS, Bemelman WA, Tanis PJ, et al. Defining indocyanine green fluorescence to assess anastomotic perfusion during gastrointestinal surgery: systematic review. *BJS Open.* 2021;5(2).
6. Driessen C, Arnardottir TH, Lorenzo AR, Mani MR. How should indocyanine green dye angiography be assessed to best predict mastectomy skin flap necrosis? A systematic review. *J Plast Reconstr Aesthet Surg.* 2020;73(6):1031-42.
7. Vahrmeijer AL, Hutteman M, van der Vorst JR, van de Velde CJ, Frangioni JV. Image-guided cancer surgery using near-infrared fluorescence. *Nat Rev Clin Oncol.* 2013;10(9):507-18.
8. Frangioni JV. In vivo near-infrared fluorescence imaging. *Curr Opin Chem Biol.* 2003;7(5):626-34.
9. Desmettre T, Devoisselle JM, Mordon S. Fluorescence properties and metabolic features of indocyanine green (ICG) as related to angiography. *Surv Ophthalmol.* 2000;45(1):15-27.
10. Johnson AC, Colakoglu S, Chong TW, Mathes DW. Indocyanine Green Angiography in Breast Reconstruction: Utility, Limitations, and Search for Standardization. *Plast Reconstr Surg Glob Open.* 2020;8(3):e2694.
11. Blanco-Colino R, Espin-Basany E. Intraoperative use of ICG fluorescence imaging to reduce the risk of anastomotic leakage in colorectal surgery: a systematic review and meta-analysis. *Tech Coloproctol.* 2018;22(1):15-23.
12. Achterberg FB, Deken MM, Meijer RPJ, Mieog JSD, Burggraaf J, van de Velde CJH, et al. Clinical translation and implementation of optical imaging agents for precision image-guided cancer surgery. *Eur J Nucl Med Mol Imaging.* 2021;48(2):332-9.
13. Goncalves LN, van den Hoven P, van Schaik J, Leeuwenburgh L, Hendricks CHF, Verduijn PS, et al. Perfusion Parameters in Near-Infrared Fluorescence Imaging with Indocyanine Green: A Systematic Review of the Literature. *Life (Basel).* 2021;11(5).
14. Dupree A, Riess H, Detter C, Debus ES, Wipper SH. Utilization of indocyanine green fluorescent imaging (ICG-FI) for the assessment of microperfusion in vascular medicine. *Innov Surg Sci.* 2018;3(3):193-201.



15. van der Vorst JR, Schaafsma BE, Verbeek FP, Swijnenburg RJ, Hutteman M, Liefers GJ, et al. Dose optimization for near-infrared fluorescence sentinel lymph node mapping in patients with melanoma. *Br J Dermatol.* 2013;168(1):93-8.
16. Pruijboom T, van Kuijk SMJ, Qiu SS, van den Bos J, Wieringa FP, van der Hulst R, et al. Optimizing Indocyanine Green Fluorescence Angiography in Reconstructive Flap Surgery: A Systematic Review and Ex Vivo Experiments. *Surg Innov.* 2020;27(1):103-19.
17. Gioux S, Choi HS, Frangioni JV. Image-guided surgery using invisible near-infrared light: fundamentals of clinical translation. *Mol Imaging.* 2010;9(5):237-55.
18. Nerup N, Andersen HS, Ambrus R, Strandby RB, Svendsen MBS, Madsen MH, et al. Quantification of fluorescence angiography in a porcine model. *Langenbecks Arch Surg.* 2017;402(4):655-62.
19. Van den Hoven P, F SW, Van De Bent M, Goncalves LN, Ruig M, S DVDB, et al. Near-infrared fluorescence imaging with indocyanine green for quantification of changes in tissue perfusion following revascularization. *Vascular.* 2021:17085381211032826.
20. Venermo M, Settembre N, Alback A, Vikatmaa P, Aho PS, Lepantalo M, et al. Pilot Assessment of the Repeatability of Indocyanine Green Fluorescence Imaging and Correlation with Traditional Foot Perfusion Assessments. *Eur J Vasc Endovasc Surg.* 2016;52(4):527-33.
21. Igari K, Kudo T, Uchiyama H, Toyofuku T, Inoue Y. Indocyanine green angiography for the diagnosis of peripheral arterial disease with isolated infrapopliteal lesions. *Ann Vasc Surg.* 2014;28(6):1479-84.
22. Nakamura M, Igari K, Toyofuku T, Kudo T, Inoue Y, Uetake H. The evaluation of contralateral foot circulation after unilateral revascularization procedures using indocyanine green angiography. *Sci Rep.* 2017;7(1):16171.
23. Ronn JH, Nerup N, Strandby RB, Svendsen MBS, Ambrus R, Svendsen LB, et al. Laser speckle contrast imaging and quantitative fluorescence angiography for perfusion assessment. *Langenbecks Arch Surg.* 2019;404(4):505-15.
24. Van Den Hoven P, Van Den Berg SD, Van Der Valk JP, Van Der Krogt H, Van Doorn LP, Van De Bogt KEA, et al. Assessment of Tissue Viability Following Amputation Surgery Using Near-Infrared Fluorescence Imaging With Indocyanine Green. *Ann Vasc Surg.* 2021.
25. Osterkamp J, Strandby R, Nerup N, Svendsen M, Svendsen L, Achiam M. Quantitative fluorescence angiography detects dynamic changes in gastric perfusion. *Surg Endosc.* 2020.



